Efficient single-photon counting at 1.55 μm by means of frequency upconversion

Marius A. Albota and Franco N. C. Wong

Research Laboratory of Electronics, Massachusetts Institute of Technology, Cambridge, Massachusetts 02139

Received January 6, 2004

We demonstrate efficient single-photon detection at 1.55 μm by means of sum-frequency mixing with a strong pump at 1.064 μm in periodically poled lithium niobate followed by photon counting in the visible region. This scheme offers significant advantages over existing InGaAs photon counters: continuous-wave operation, higher detection efficiency, higher counting rates, and no afterpulsing. We achieved single-photon upconversion efficiency of 90% at 21.6 W of circulating power in a resonant pump cavity with a 400-mW Nd:YAG laser. We observed high background counts at strong circulating pump powers due to efficient upconversion of pump-induced fluorescence photons.

OCIS codes: 270.0270, 030.5260, 270.5570.

Many quantum optics applications, such as quantum cryptography,[1–3] cannot take full advantage of the inherently low transmission loss of optical fibers and the atmosphere at 1.55 μm because good single-photon detectors in that spectral region are not currently available. Efficient single-photon counting near 1.5 μm would also be useful in traditional applications such as classical optical communication, imaging, and astronomy. Recent studies on 1.3–1.6-μm single-photon counting devices employ InGaAs avalanche photodiodes (APDs) that are biased above the breakdown voltage, cooled, and operated in the Geiger mode.[4–6] The reported efficiencies are generally in the 15–25% range, depending on the operating temperature and the associated trade-offs in dark counts and counting rates. Since InGaAs devices cannot be operated continuously because of severe afterpulsing, gated passively quenched operation is typically used. In contrast, Si APD single-photon counting modules (SPCMs) are commercially available and have desirable characteristics, such as high quantum efficiencies (>70%) and low dark count rates (<100/s). Moreover, since afterpulsing is not a problem, these SPCMs can be operated in cw mode at rates as high as 10 MHz. Here we report efficient single-photon detection at 1.55 μm by means of sum-frequency generation followed by direct detection in the visible region with a Si SPCM. Although this basic idea was demonstrated for squeezed states of light,[7] it was only recently implemented for single photons.[8]

Consider the sum-frequency generation of the output field at ω_2 in a nonlinear $\chi^{(2)}$ crystal from a strong pump field at ω_p and a weak input field at ω_1. Treating the pump classically, the solution to the coupled-mode equations for the phase-matched interaction is

$$\hat{a}_1(L) = \cos(|gE_p|L)\hat{a}_1(0) - \sin(|gE_p|L)\hat{a}_2(0), \quad (1)$$

$$\hat{a}_2(L) = \sin(|gE_p|L)\hat{a}_1(0) + \cos(|gE_p|L)\hat{a}_2(0), \quad (2)$$

where $\hat{a}_i$ is the single-mode annihilation operator, L is the crystal length, g is the nonlinear interaction strength, and E_p is the pump electric field. Frequency translation of any quantum state at ω_1 to the same quantum state at ω_2 with unity efficiency is possible, even at the single-photon level, if $|gE_p|L = \pi/2$. More importantly, the technique is suitable for converting entangled photons that are generated at one frequency to a different frequency with quantum-state preservation. This makes upconversion of individual photons useful in novel applications such as long-distance quantum entanglement distribution and quantum teleportation.[9] We note that for classical applications $\hat{a}_i$ is replaced by the corresponding electric field E_i, and the upconversion results are unchanged: A weak input probe at ω_1 can be completely converted to an output signal at ω_2.

The sum-frequency generation technique is characterized by the upconversion efficiency $\eta = N_2(L)/N_1(0)$, where $N_i = \langle \hat{a}_i^\dagger \hat{a}_i \rangle_T$ is the mean photon number at ω_i in measurement time T. For vacuum input at ω_2, $\eta = \sin^2(|gE_p|L)$, which can be written functionally as

$$\eta = \sin^2[(\pi/2)(P_p/P_{\max})^{1/2}], \quad (3)$$

where P_p is the input pump power to the nonlinear crystal, and $P_{\max}$ is the pump power required to achieve unity conversion efficiency and is given by

$$P_{\max} = \frac{c\epsilon_0 n_1 n_2 \lambda_1 \lambda_2 \lambda_p}{128 d_{\text{eff}}^2 L \bar{h}_m(B, L/b_p)}. \quad (4)$$

Here d_{eff} is the effective nonlinear coefficient, $\bar{h}_m$ is the reduction factor for focused Gaussian beams with a double refraction parameter $B = 0$ and a focusing parameter L/b_p, and b_p is the confocal parameter for the mode-matched interaction. For $\lambda_{1,2,p} = 1.548$, 0.631, and 1.064 μm, respectively, using periodically poled lithium niobate (PPLN) with $d_{\text{eff}} \approx 14$ pm/V and $L/b_p = 1$ ($\bar{h}_m = 0.776$), we obtain $P_{\max} \approx 17$ W. We note that the required pump power can be further reduced using a PPLN waveguide but at the expense of waveguide and coupling losses that limit the maximum achievable upconversion efficiency.

To implement our cw upconversion scheme in bulk PPLN with the available 400-mW Nd:YAG laser, we resonated the cw pump in a ring cavity. The setup is shown in Fig. 1. The cavity was single pass for the input probe and output signal to minimize the

0146-9592/04/131449-03$15.00/0

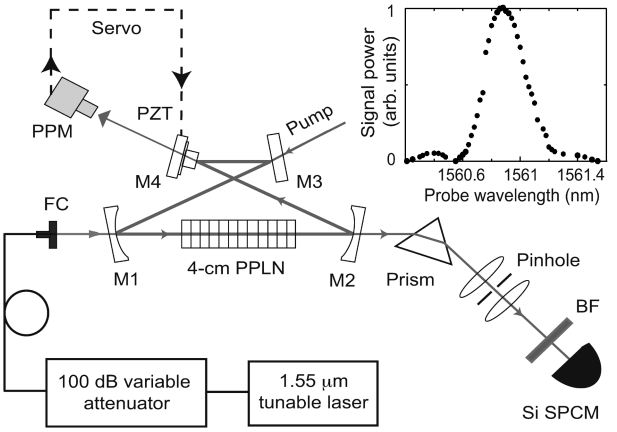

Fig. 1. Experimental setup for single-photon detection at 1.55 μm by means of upconversion. FC, fiber-optic collimator; BF, 10-nm interference filter at 633 nm and 1064-nm HR mirror; PPM, pump power monitor; PZT, piezoelectric transducer. Inset, wavelength phase-matching curve at a PPLN temperature of 229 °C (~0.3-nm bandwidth).

insertion loss and to allow for both cw and pulsed upconversion. It also imposed a well-defined spatial mode that simplified pump–probe mode matching and efficiency optimization. We housed the 40-mm-long PPLN crystal in an oven set at ~197 °C for first-order, type I, quasi-phase-matched sum-frequency generation of $\lambda_2 = 631$ nm from inputs at $\lambda_1 = 1548$ nm and $\lambda_p = 1064$ nm. The oven was controlled to within ± 0.1 °C, which is less than the PPLN temperature phase-matching bandwidth of 1 °C. The crystal had six gratings (11–12 μm; 0.2-μm step) that allowed a wide range of input wavelengths. Together with a temperature range of 140–230 °C and at a fixed λ_p, this setup can accommodate any input wavelength λ_1 in the 1.52–1.66-μm range with a PPLN temperature coefficient of ~0.35 nm/°C. The inset in Fig. 1 shows the wavelength-tuning curve for the 11.2-μm grating of the crystal at 229 °C, indicating a 0.3-nm phase-matching bandwidth, which is in agreement with the value calculated from the Sellmeier equations for PPLN. The crystal was antireflection coated at the pump, input, and output wavelengths. The 75-mm radius-of-curvature mirror M1 (M2) served as the input (output) for the probe (signal) and was coated for high reflection (HR) at λ_p and high transmission at λ_1 (λ_2). M3 was a 2.15% flat coupler for the pump, and the leakage through the flat HR mirror M4 ($T \sim 0.02\%$) was used to monitor P_p with an InGaAs detector. We measured a cavity finesse of ~210 and obtained a maximum circulating power $P_p \approx 23$ W with the 400-mW pump laser.

The pump focus at the center of the crystal had a beam waist of ~55 μm (with ~10% difference between the sagittal and tangential waists). We mounted M4 on a piezoelectric transducer to scan the cavity length and servo locked the cavity to the pump transmission peak with a dither-and-lock method. The servo loop had a unity-gain frequency of ~20 kHz, and we were able to maintain a highly stable cavity lock for many minutes with a rms error of less than 1% in P_p. At the highest pump powers we observed significant thermal hysteresis due to the high circulating power and heating of the crystal, and the servo became slightly less stable. The probe was supplied by a fiber-coupled tunable Fabry–Perot laser and attenuated with a 100-dB fiber-optic variable attenuator that was calibrated with wavelength-flattened inline taps and an ultrasensitive fiber-coupled InGaAs detector with 10-fW sensitivity. The probe beam was collimated for propagation through free space and mode matched into the cavity with a beam waist of ~67 μm at the center of the crystal. We measured the actual beam waists with a beam scanner and monitored the horizontally polarized input power to the cavity.

Measurements of the weak-probe upconversion efficiency were done with 284 μW of input power at $\lambda_1 = 1548.47$ nm. The cw output at 631 nm was filtered with a 1.06-μm HR mirror and a 10-nm interference filter centered at 633 nm. The imaging optics and spectral filters had an overall transmission of 68%, and the upconverted light was detected with a large-area Si photodiode. We aligned and calibrated our system with a 633-nm He–Ne laser and *in situ* with the upconverted signal. Figure 2 shows the intrinsic upconversion efficiency as a function of P_p, and the solid curve is a fit to the data with the functional form of Eq. (3). As expected, at low pump powers the efficiency is linearly proportional to P_p. At high pump powers the efficiency saturates as it approaches unity. The upconversion efficiency reaches 93% at $P_p = 23$ W, with an estimated uncertainty of $\pm 3\%$ due to calibration accuracies. We were unable to reach unity efficiency due to insufficient pump power; from the fit in Fig. 2 we estimate $P_{\max} = 31$ W. This higher-than-estimated $P_{\max}$ is probably caused by a smaller d_{eff} (PPLN quality) and suboptimal mode matching between the probe and the slightly astigmatic pump.

For upconversion at the single-photon level we attenuated the input probe power to 0.095 photon/μs and sent the signal to a Si SPCM with a nominal quantum efficiency of 65%. The output imaging system, shown in Fig. 1, was more elaborate than that used for the weak-probe measurements because it was essential to minimize stray and leakage pump light from reaching the Si SPCM. Additional filtering

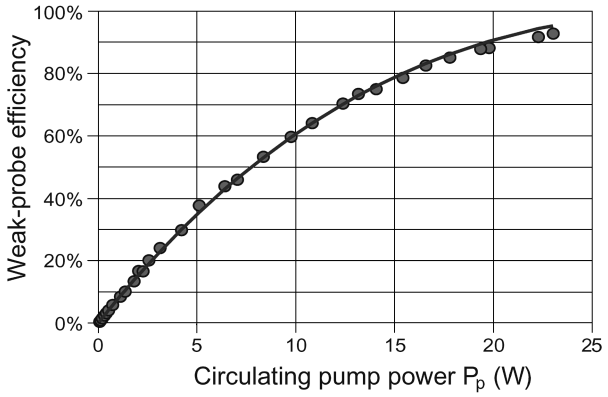

Fig. 2. Weak-probe cw upconversion efficiency as a function of P_p. Filled circles, experimental data; solid curve, functional fit of Eq. (3) with $P_{\max} = 31$ W.

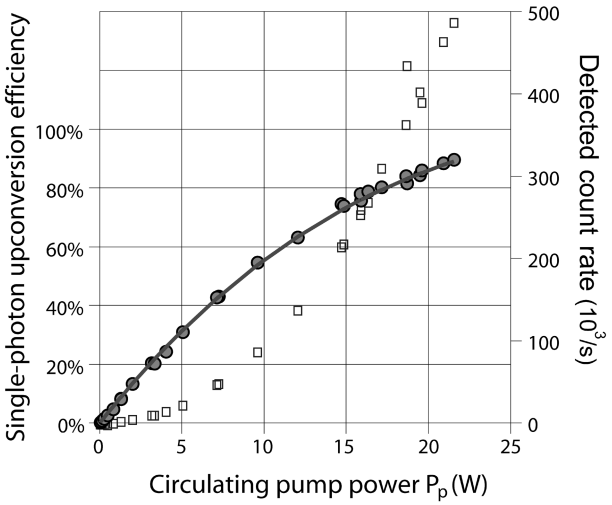

Fig. 3. Single-photon cw upconversion efficiency as a function of P_p (filled circles). Solid curve, functional fit of Eq. (3) with $P_{\max} = 35$ W. Right axis, upconverted signal counts (filled circles) and background counts (open squares) as a function of P_p.

included a Brewster-angled dispersing prism and a 100-μm pinhole used as a spatial filter to block the weak second-harmonic light and the off-axis upconverted light. The overall transmission of the imaging system was ~58%. With the cavity locked we measured the total counts and, by blocking the probe input, the background counts as a function of P_p. We obtained the upconverted signal counts by subtracting the background counts from the total counts. Figure 3 shows the intrinsic single-photon upconversion efficiency (filled circles), indicating a maximum of 90% at $P_p = 21.6$ W. The functional fit of Eq. (3) is also plotted, as a solid curve, again showing excellent agreement with the data. At high P_p we observed significant background counts that included detector dark counts and stray light of ~300/s. Figure 3 also shows the upconverted signal counts (filled circles) and the background counts (open squares) versus the circulating pump power. Crystal heating at the highest P_p caused a small rise in the crystal temperature, which under cw operation was compensated by a slight adjustment to the probe wavelength (a maximum of <0.2 nm) or the oven set point to maintain peak upconversion efficiency. We note that the fit yields $P_{\max} = 35$ W, which is higher than that obtained in Fig. 2, probably as a result of pump–probe misalignment. We also measured the depletion of the weak probe with the setup shown in Fig. 1 using an InGaAs photodiode and obtained a maximum depletion of 89% at $P_p \approx 21$ W, which is in good agreement with the upconversion measurements.

The large background counts that appear at high pump powers can be a severe limitation. These counts can be further reduced by use of narrower spatial and spectral filtering and are less of a problem for coincidence counting applications: A 1-ns coincidence window yields a maximum probability of a background count of only 4.6×10^{-4}. It is, however, possible to eliminate these background counts. We note that the background photons are due to a two-step cascaded process: pump-induced fluorescence and (non-phase-matched) parametric fluorescence at the probe wavelength λ_1 followed by upconversion from λ_1 to λ_2. If we were to choose the pump wavelength to be longer than the probe wavelength, $\lambda_p > \lambda_1$, such that the energy of a pump photon is lower than the energy of the probe photon, the first step, generating the fluorescence photons, can be eliminated. We believe this is an important consideration when applying this technique for low-noise detection of infrared photons.

In summary, we have demonstrated efficient cw wavelength-tunable detection of 1.55-μm photons by means of sum-frequency mixing in bulk PPLN. Insufficient pump power and suboptimal mode matching limit our maximum upconversion efficiency to ~90%. Our scheme is also suitable for pulsed inputs as long as the pulse bandwidth is narrower than the phase-matching bandwidth of the PPLN crystal. Such pulses would permit the loading of trapped-atom quantum memories with typical bandwidths of 50 MHz.[9] The setup also acts as a narrowband detection filter with a 0.3-nm passband. By combining a 90% efficient upconverter with a 65% efficient Si SPCM, we achieved cw counting of 1.55-μm photons at megahertz rates with no afterpulsing and an overall efficiency of 59%, which is much higher than that of current InGaAs detectors. Eliminating most of the background counts will make this technique an even more attractive option for many quantum and classical applications.

We thank J. H. Shapiro for useful discussions and C. E. Kuklewicz for help with data acquisition. This work was supported by the Department of Defense Multidisciplinary University Research Initiative program under Army Research Office grant DAAD-19-00-1-0177, Defense University Research Instrumentation Program instrumentation grant DAAD-19-01-1-0355, and the Massachusetts Institute of Technology Lincoln Laboratory. M. A. Albota's e-mail address is albota@mit.edu.

References

1. D. Stucki, N. Gisin, O. Guinnard, G. Ribordy, and H. Zbinden, New J. Phys. **4,** 41.1 (2002).
2. D. S. Bethune and W. P. Risk, New J. Phys. **4,** 42.1 (2002).
3. R. J. Hughes, J. E. Nordholt, D. Derkacs, and C. G. Peterson, New J. Phys. **4,** 43.1 (2002).
4. D. Stucki, G. Ribordy, A. Stefanov, H. Zbinden, J. G. Rarity, and T. Wall, J. Mod. Opt. **48,** 1967 (2001).
5. E. J. Mason, M. A. Albota, F. König, and F. N. C. Wong, Opt. Lett. **27,** 2115 (2002).
6. D. S. Bethune, W. P. Risk, and G. W. Pabst, *arXiv.org e-Print archive*, quant-ph/0311112, November 17, 2003, http://arxiv.org/abs/quant-ph/0311112.
7. J. M. Huang and P. Kumar, Phys. Rev. Lett. **68,** 2153 (1992).
8. M. A. Albota and F. N. C. Wong, in *Quantum Electronics and Laser Science (QELS)*, Vol. 89 of OSA Trends in Optics and Photonics Series (Optical Society of America, Washington, D.C., 2003), postdeadline paper QThPDB11.
9. J. H. Shapiro, New J. Phys. **4,** 47.1 (2002).